Electronic Supplementary Information

Photoelectric Effect of Hybrid Ultraviolet-Sensitized Phototransistors from N-type Organic Semiconductors and All-Inorganic Perovskite Quantum Dots Photosensitizer

Shao-Huan Hong,‡[a] Shakil N. Afraj,‡[b] Ping-Yu Huang,[b] Yi-Zi Yeh,[b] Shih-Huang Tung,[c] Ming-Chou Chen,[b] and Cheng-Liang Liu[d]*

a. Department of Chemical and Materials Engineering, National Central University, Taoyuan 32001, Taiwan.

b. Department of Chemistry, National Central University, Taoyuan 32001, Taiwan.

c. Institute of Polymer Science and Engineering, National Taiwan University, Taipei 10617, Taiwan.

d. Department of Material Science and Engineering, National Taiwan University, Taipei 10617, Taiwan. E-mail: liucl@ntu.edu.tw

‡ These Authors Contributed equally to this work.

Materials: All chemicals and anhydrous solvents were used as received without further purification.

Characterization: Morphology and electron diffraction of $CsPbBr_3$ QDs were evaluated using a JEOL JEM-2100 transmission electron microscope (TEM), operating at an accelerating voltage of 200 kV. X-ray diffraction (XRD) patterns of $CsPbBr_3$ QDs samples were determined on a Bruker Advance D8 diffractometer equipped with Cu Kα radiation (λ= 1.5416 Å). X-ray photoelectron spectroscopies (XPS; Thermo VG-Scientific Sigma Probe) were used to probe the elemental composition of QDs. The UV-Vis spectra were obtained on a HITACHI U-4100 spectrometer. Thin film photoluminescence (PL) spectra were measured using Raman Spectrometer and Picosecond Pulse Laser System (Uni-RAM MGL-FN-532). The ionization energy was determined from the photoelectron emission yield measured by a Photon Electron Spectroscopy in Air (PESA) system (RIKEN KEIKI AC-2) operating at room temperature. Surface morphologies of the blend thin films were determined by an atomic force microscopy (Seiko SPA-400) under ambient condition. A time-of-flight secondary ion mass spectrometry (TOF-SIMS) spectrometer (ION-TOF, TOF-SIMS V) was utilized to depth-profile the blend films. Grazing incidence X-ray diffraction (GIXRD) measurements were performed at beamline TLS 13A1/17A1/23A1 at National Synchrotron Radiation Research Center (NSRRC) of Taiwan.

Table S1. Key figures of merit of perovskite QD-containing hybrid phototransistor.

Hybrid Materials	Photoactive layer	R [A W^{-1}]	S	D [Jones]	Ref
$CsPbBr_3$ QD/DNTT	bilayer	1.7×10^4	8.1×10^4	2×10^{14}	[1]
DPP-DTT/$CsPbI_3$ QD	bilayer	110	6×10^3	2.9×10^{13}	[2]
PQT-12:$CsPbBr_3$ QD	blend	22.18	-	-	[3]
C8-BTBT:$CH_3NH_3PbI_3$ NP[a]	blend	1.72×10^4	-	2.09×10^{12}	[4]
DTTQ:$CsPbBr_3$ QD	blend	7.1×10^5	1.8×10^4	3.6×10^{13}	this work

[a)](NP: nanoparticle)

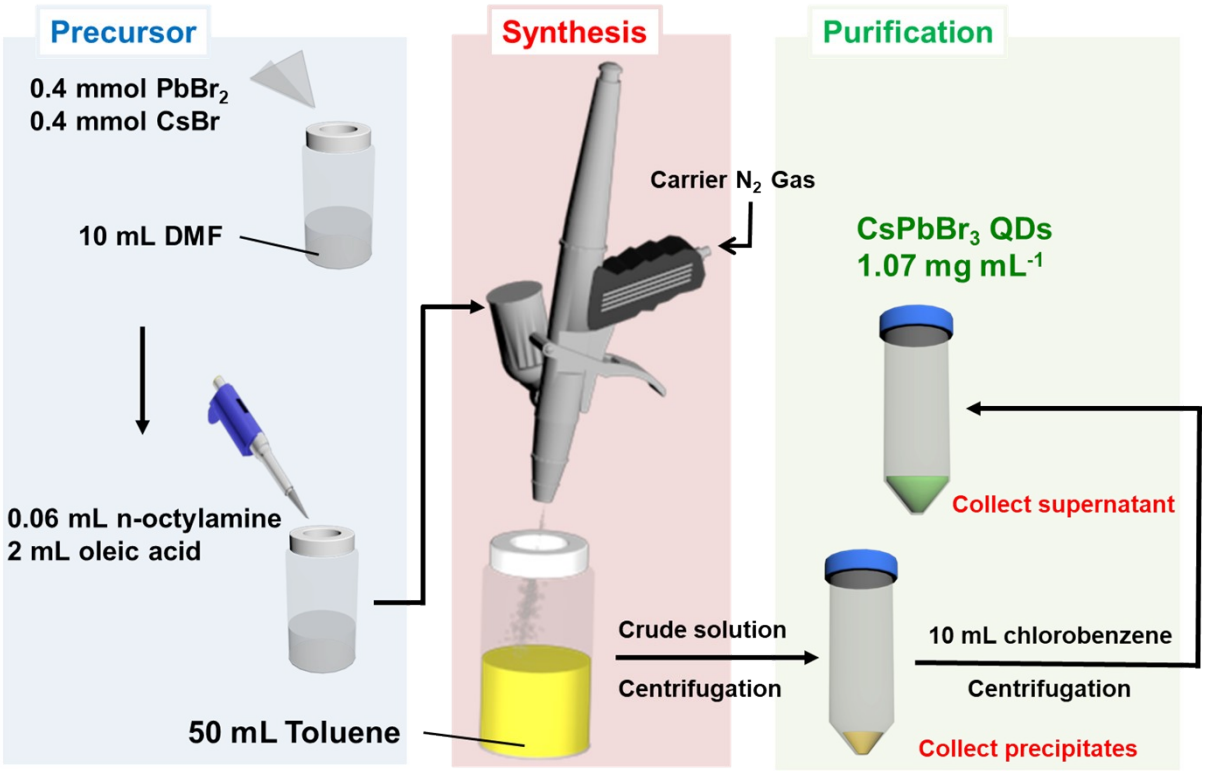

Fig. S1 The schematics of $CsPbBr_3$ QDs preparation.

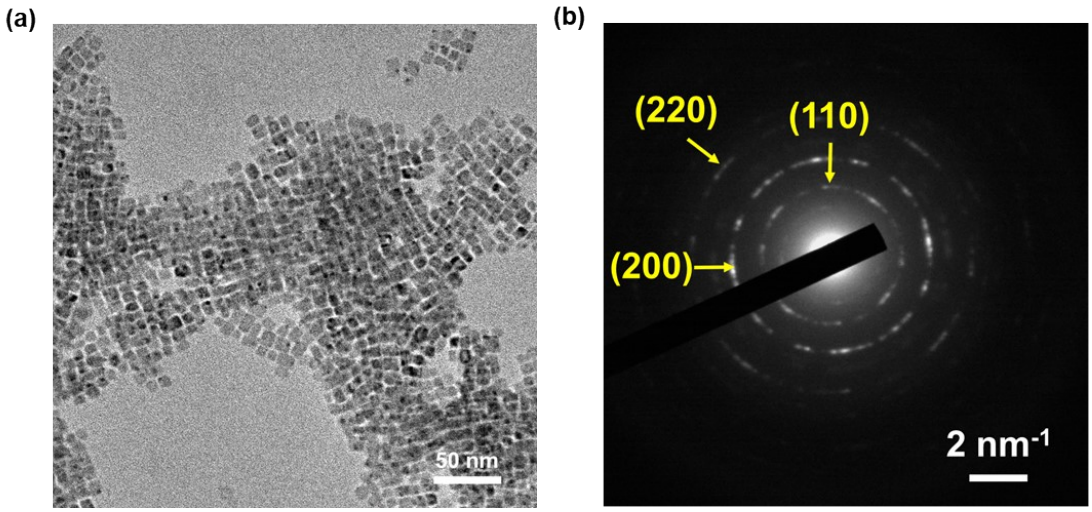

Fig. S2 Characterization of $CsPbBr_3$ QDs: (a) TEM image and (b) SAED patterns.

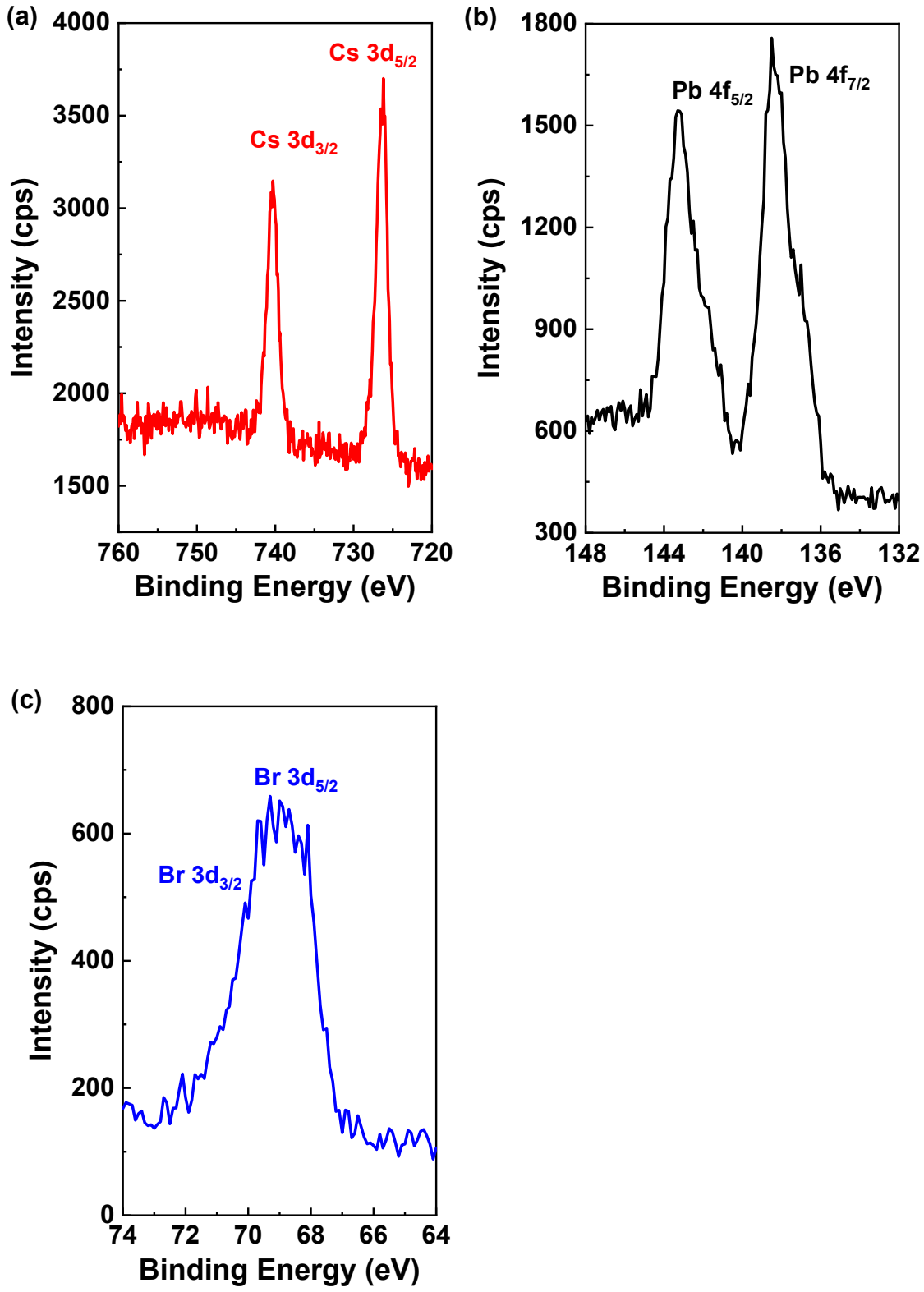

Fig. S3 High resolution of XPS spectra for (a) Cs 3d, (b) Pb 4f, and (c) Br 3d of $CsPbBr_3$ perovskite QDs.

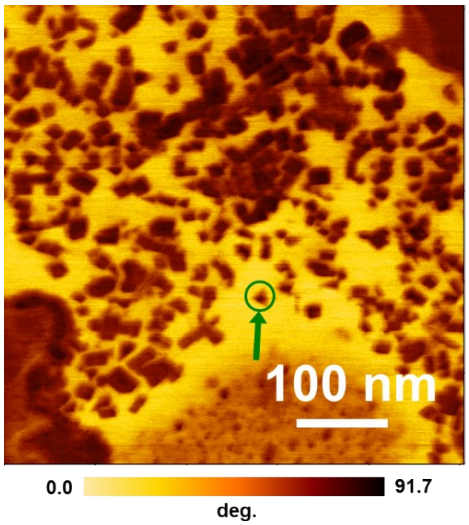

Fig. S4 AFM phase image of solution-sheared DTTQ:QD (3:7) film.

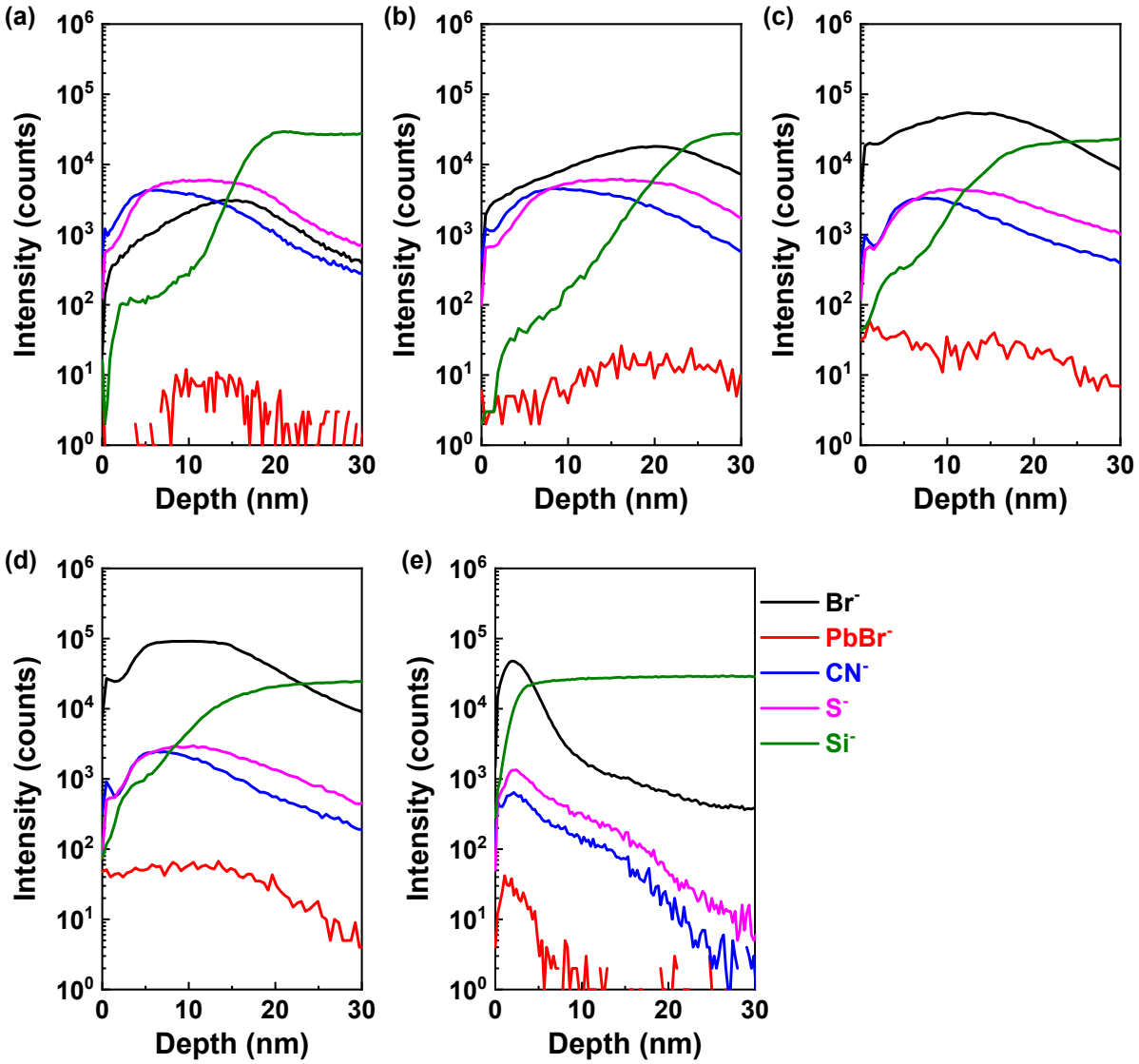

Fig. S5 TOF-SIMS depth profile of solution-sheared DTTQ:QD (a) (9:1), (b) (7:3), (c) (5:5), (d) (3:7), and (e) (1:9) films.

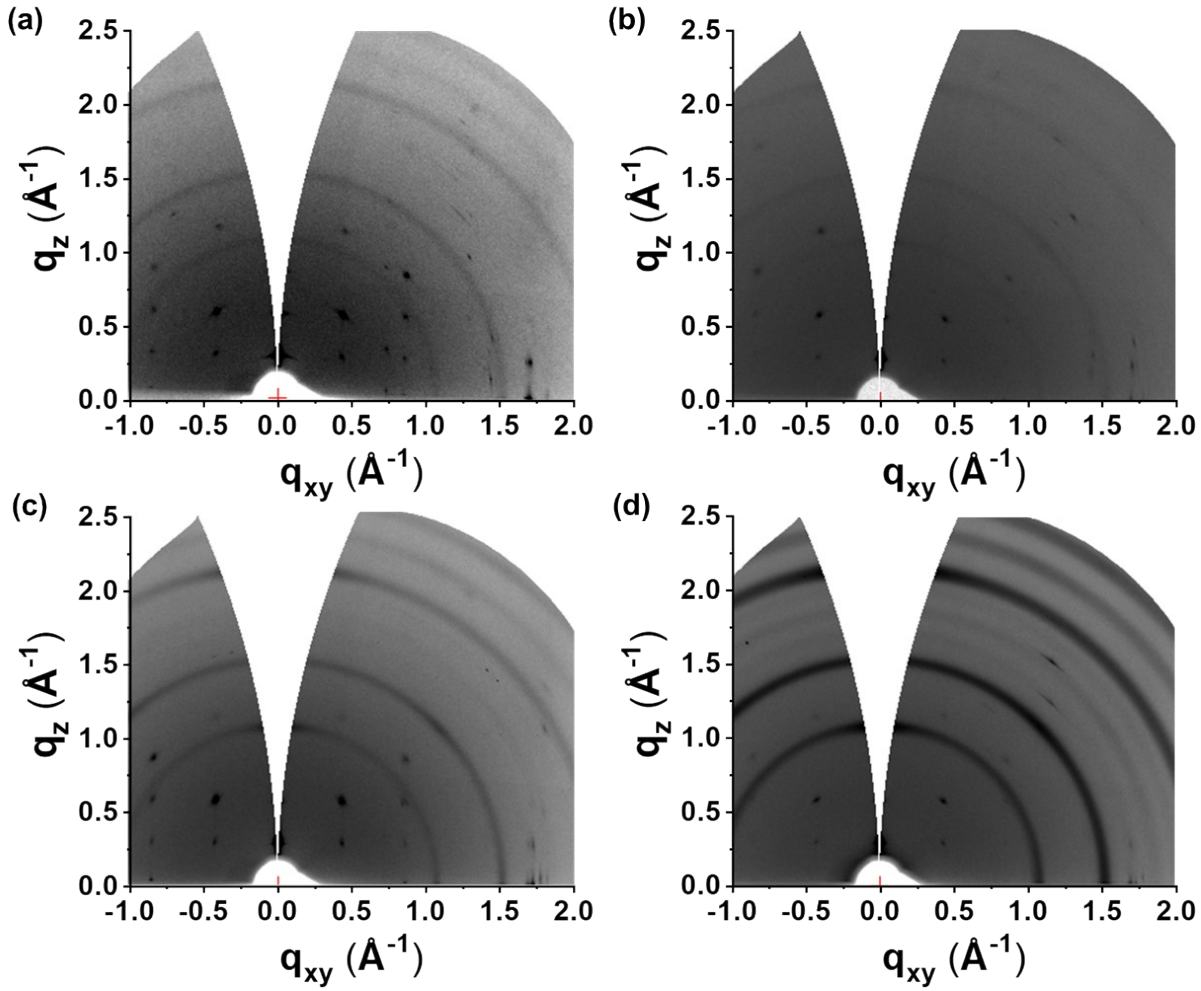

Fig. S6 2D GIXRD profile of solution-sheared DTTQ:QD (a) (9:1), (b) (7:3), (c) (5:5), and (d) (1:9) films.

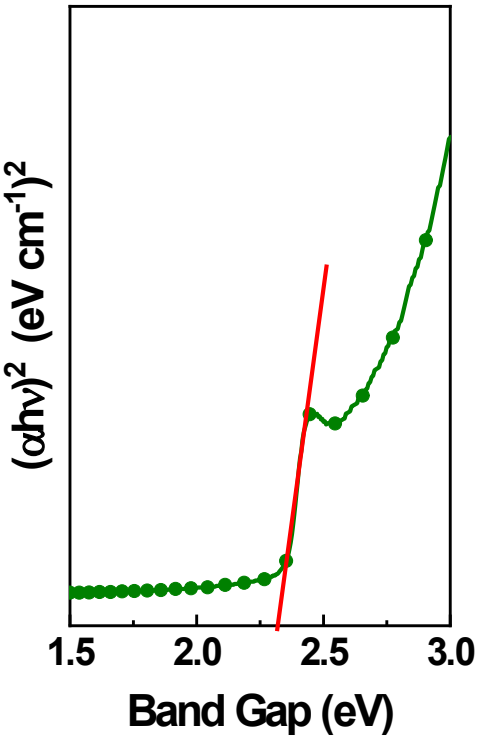

Fig. S7 Tauc plot for bandgap estimation of $CsPbBr_3$ QDs film.

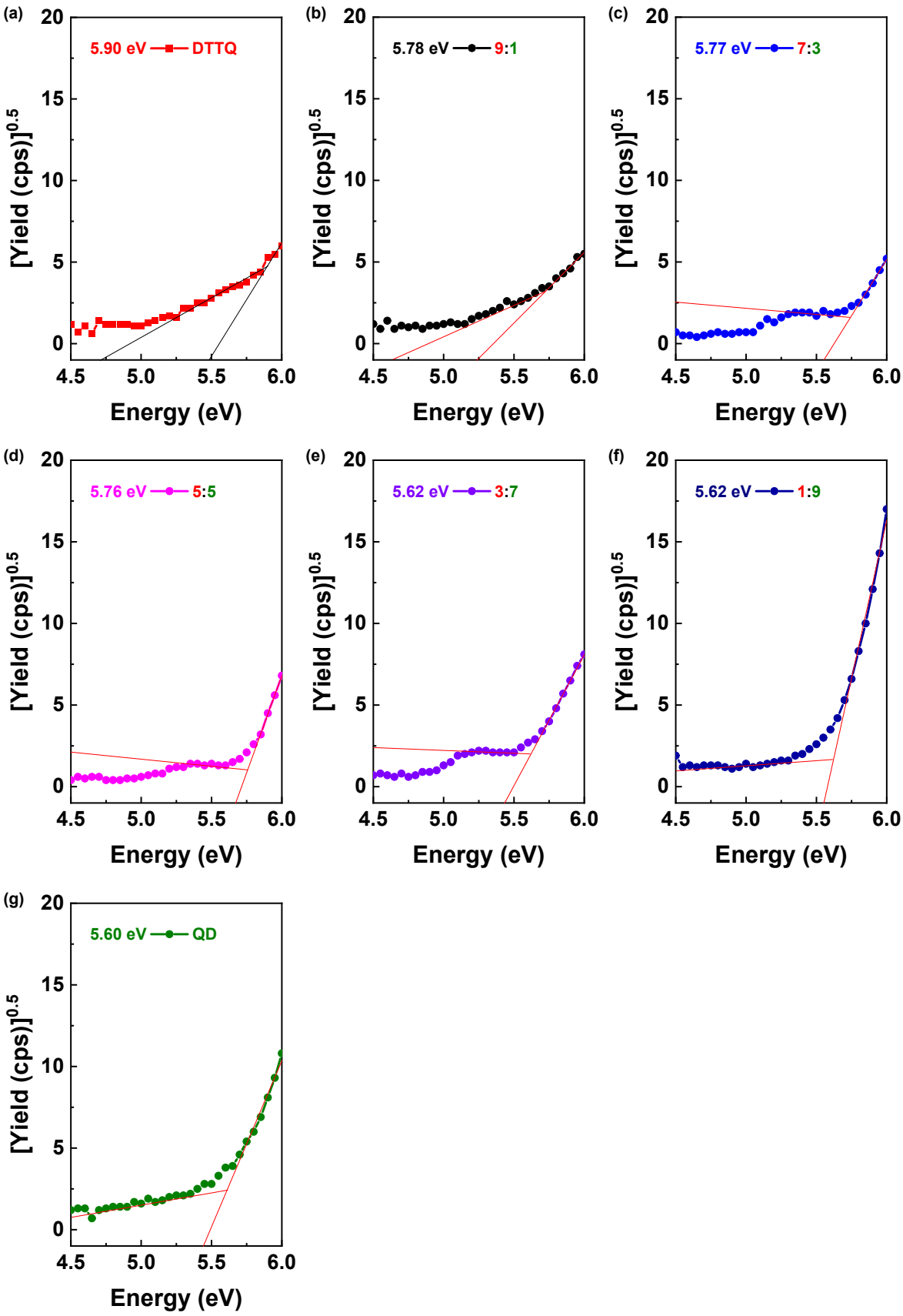
(a)
5.90 eV DTTQ
(b)
5.78 eV 9:1
(c)
5.77 eV 7:3
(d)
5.76 eV 5:5
(e)
5.62 eV 3:7
(f)
5.62 eV 1:9
(g)
5.60 eV QD
[Yield (cps)]^0.5
Energy (eV)
0
5
10
15
20
4.5
5.0
5.5
6.0

Fig. S8 PESA studies carried out for HOMO of solution-sheared DTTQ (a), and E_v of $CsPbBr_3$ QDs (g) and those of DTTQ:QD (b) (9:1), (c) (7:3), (d) (5:5), (e) (3:7), and (f) (1:9) films. A small hump near 5.0 eV can be observed since the work function of SiO_2 is around 5.0 eV.

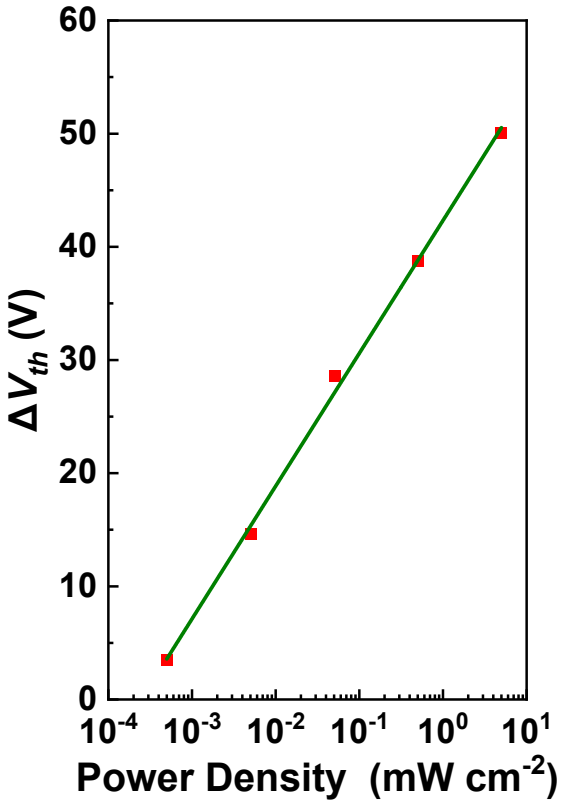

Fig. S9 Shift in the threshold voltage (ΔV_{th}) of DTTQ:QD (3:7) hybrid phototransistor as a function of illumination light intensity.

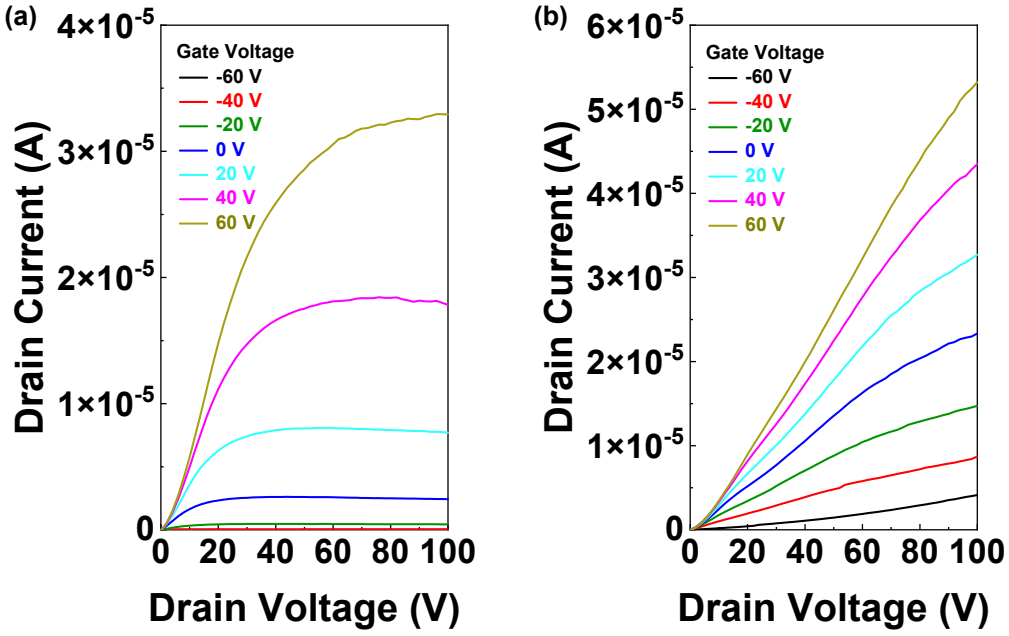

Fig. S10 Output characteristics of DTTQ:QD (3:7) hybrid phototransistor (a) in dark and (b) under illumination.

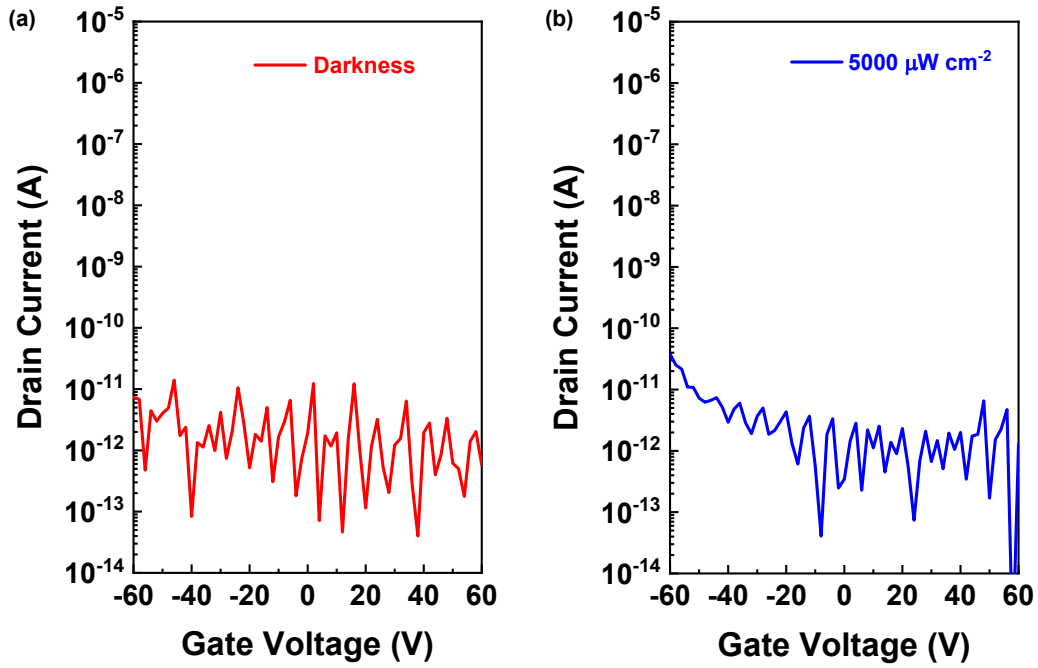

Fig. S11 Transfer characteristics of QD phototransistor (a) in dark and (b) under illumination.

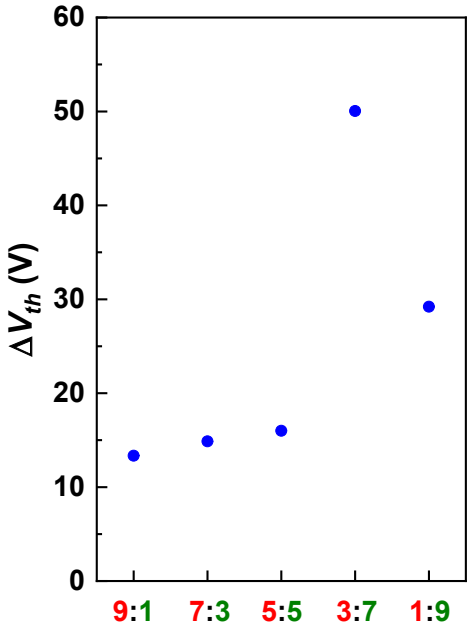

Fig. S12 Shift in the threshold voltage (ΔV_{th}) of DTTQ:QDs (9:1), (7:3), (5:5), (3:7) and (1:9) phototransistor between the dark and illuminated (light intensity of 5000 µW cm^{-2}) condition.

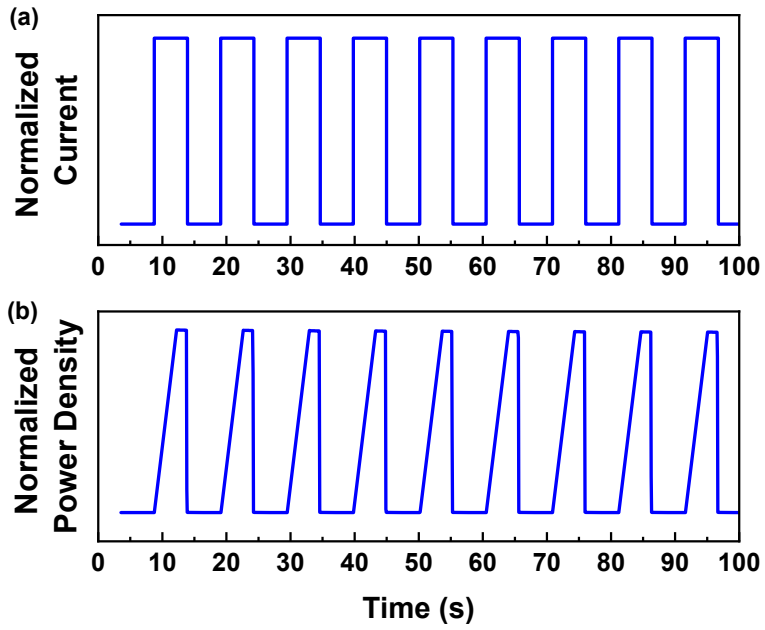

Fig. S13 Actual response of (b) the incident light pulse (normalized), as powered by (a) electrical pulse.

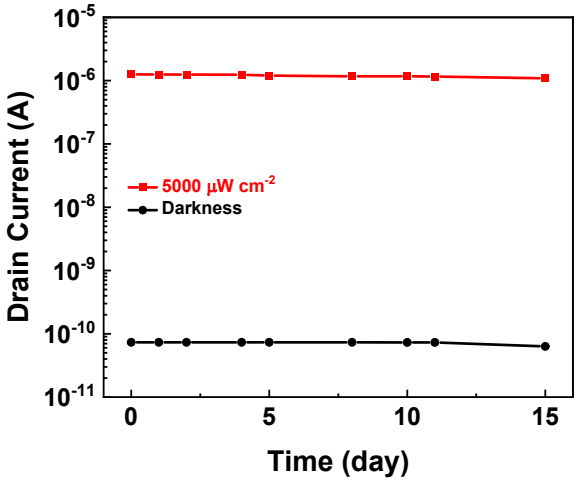

Fig. S14 Long term stability test of DTTQ:QD (3:7) hybrid phototransistor: The I_{illum} and I_{dark} as a function of time.

Reference

1. Y. Chen, Y. Chu, X. Wu, W. Ou-Yang and J. Huang, *Adv. Mater.*, 2017, **29**, 1704062.
2. C. Zou, Y. Xi, C.-Y. Huang, E. G. Keeler, T. Feng, S. Zhu, L. D. Pozzo and L. Y. Lin, *Adv. Opt. Mater.*, 2018, **6**, 1800324.
3. K. Wang, S. Dai, Y. Zhao, Y. Wang, C. Liu and J. Huang, *Small*, 2019, **15**, 1900010.
4. X. Xu, W. Deng, X. Zhang, L. Huang, W. Wang, R. Jia, D. Wu, X. Zhang, J. Jie and S.-T. Lee, *ACS Nano*, 2019, **13**, 5910-5919.